# VELO Toy Model: Track Reconstruction Study

Sparse and Dense Event Analysis

Parameter Optimization and Performance Characterization

George William Scriven

December 2025

**Abstract**

This report documents a comprehensive study of track reconstruction performance using the VELO toy model with a Hamiltonian-based segment matching algorithm. We investigate the effects of hit resolution ($\sigma_{\text{res}}$), multiple scattering ($\sigma_{\text{scatt}}$), scale factor ($n$), and threshold function (step vs. erf) on reconstruction efficiency and ghost rate. Three experimental runs (Runs 8, 9, and 10) were conducted, analyzing over 3000 events across sparse (10 tracks) and dense (100 tracks) configurations. Key findings include: (1) optimal performance at $\sigma_{\text{res}} \leq 10$ $\mu$m and $\sigma_{\text{scatt}} \leq 0.2$ mrad, (2) scale factor $n = 3$–$5$ provides best efficiency-ghost trade-off, and (3) performance degradation with increasing multiple scattering is driven by increased track angular density. The validator uses a completeness threshold of 70% as specified in the LHCb instructions.

## Contents

# 1 Introduction

## 1.1 Motivation

The LHCb VELO (VErtex LOcator) detector requires efficient track reconstruction algorithms capable of handling high track multiplicities. This study uses a toy model to investigate the fundamental limits and parameter dependencies of a Hamiltonian-based track reconstruction approach.

## 1.2 The VELO Toy Model

The toy model simulates:

- A simplified detector geometry with multiple parallel sensor planes
- Particle tracks traversing the detector with configurable multiplicity
- Hit position smearing based on measurement resolution ($\sigma_{\text{res}}$)
- Multiple scattering effects parameterized by $\sigma_{\text{scatt}}$

## 1.3 Hamiltonian Track Reconstruction

Track reconstruction is formulated as an optimization problem using a Hamiltonian approach:

$$H = -\sum_{\text{segments}} w_{ij} \cdot x_i \cdot x_j \tag{1}$$

where $w_{ij}$ represents the compatibility weight between segment pairs $(i, j)$ and $x_i \in \{0, 1\}$ indicates segment selection.

### 1.3.1 Angular Threshold

The segment compatibility is determined by the inter-segment angle $\theta$ compared to a threshold $\varepsilon$:

$$\varepsilon = \sqrt{\theta_s^2 + \theta_r^2 + \theta_{\text{min}}^2} \tag{2}$$

where:

- $\theta_s = n \cdot \sigma_{\text{scatt}}$ is the multiple scattering contribution
- $\theta_r = \arctan(n \cdot \sigma_{\text{res}}/\Delta z)$ is the resolution contribution
- $\theta_{\text{min}} \approx 15$ $\mu$rad is a minimum threshold
- $n$ is the scale factor

### 1.3.2 Threshold Functions

Two threshold functions are compared:

**Step function:**

$$w(\theta) = \begin{cases} 1 & \text{if } |\theta| \leq \varepsilon \\ 0 & \text{otherwise} \end{cases} \tag{3}$$

**Error function (erf):**

$$w(\theta) = \frac{1}{2}\left(1 + \text{erf}\left(\frac{\varepsilon - |\theta|}{\theta_d\sqrt{2}}\right)\right) \tag{4}$$

where $\theta_d$ is the erf smoothing parameter (erf_sigma).

# 2 Experimental Setup

## 2.1 Parameter Space

Three comprehensive parameter scans were conducted:

Table 1: Parameter ranges for each experimental run

| Parameter | Runs 8 | Runs 9 | Runs 10 |
|---|---|---|---|
| $\sigma_{\text{res}}$ ($\mu$m) | 1, 10 | 1–200 | 0, 10, 20, 50 |
| $\sigma_{\text{scatt}}$ (mrad) | 0.01 | 0.001–1 | 0, 0.1, 0.2, 0.3, 0.5, 1.0 |
| Scale $n$ | 2–10 | 2–10 | 3, 4, 5 |
| erf_sigma | $10^{-6}$–$10^{-3}$ | $10^{-6}$–$10^{-3}$ | $10^{-4}$ |
| Track density | sparse (10), dense (100) | sparse (10), dense (100) | sparse (10) |
| Threshold | step, erf | step, erf | step |
| Events per config | 10 | 10 | 50–500 |

## 2.2 Validation Metrics

Track reconstruction quality is evaluated using metrics defined in the LHCb instructions:

**Completeness:** Fraction of truth track hits found in reconstructed track

$$\text{Completeness} = \frac{N_{\text{shared}}}{N_{\text{truth}}} \tag{5}$$

**Track Classification:**

- **GOOD**: Reconstructed track with completeness $\geq 70\%$
- **GHOST**: Reconstructed track with completeness $< 70\%$

**Efficiency:**

$$\text{Efficiency} = \frac{N_{\text{GOOD}}}{N_{\text{truth}}} \tag{6}$$

**Ghost Rate:**

$$\text{Ghost Rate} = \frac{N_{\text{GHOST}}}{N_{\text{reconstructed}}} \tag{7}$$

## 2.3 Computing Infrastructure

All simulations were executed on the Nikhef HTCondor cluster with:

- Batch job submission for parallel parameter scanning
- Event stores saved as compressed pickle files
- Post-processing aggregation of metrics

# 3 Runs 8: Scale Factor and ERF Sigma Study

## 3.1 Objectives

Runs 8 investigated:

1. The effect of scale factor $n$ on reconstruction performance

2. Comparison of step vs. erf threshold functions
3. Independence of step function results from erf_sigma parameter
4. Performance difference between sparse (10 tracks) and dense (100 tracks) events

## 3.2 Key Results

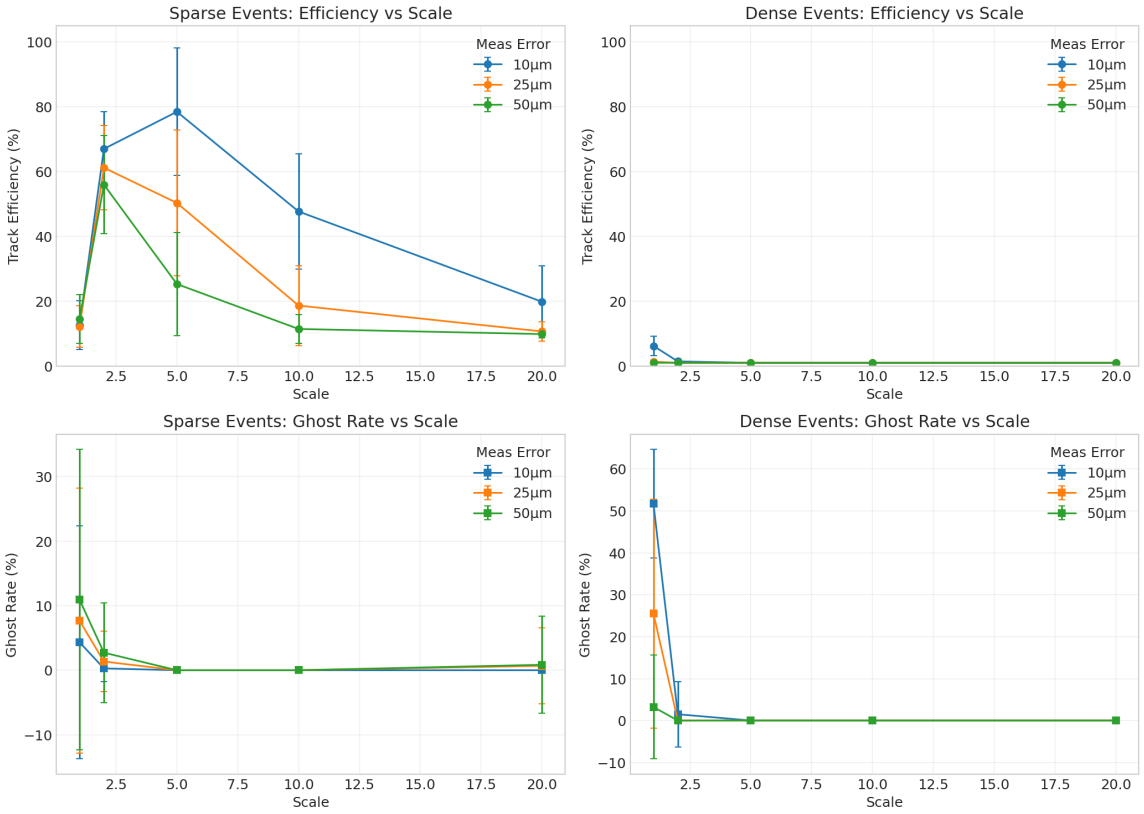


Figure 1: Runs 8: Effect of scale factor on track efficiency and ghost rate for sparse and dense events

### 3.2.1 Step Function Independence Verification

A critical verification was performed to confirm that step function results are independent of the erf_sigma parameter:

> *Result: Step function gives IDENTICAL results for all erf_sigma values, with maximum efficiency variation* $< 10^{-10}$ *across the same (parameters, repeat) combinations.*

This confirms correct implementation of the threshold logic.

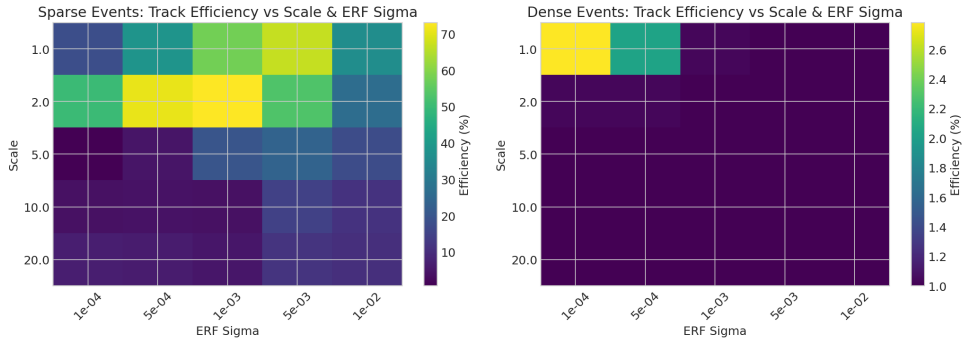


Figure 2: Runs 8: ERF sigma effect on track efficiency (confirms step function independence)

### 3.2.2 Sparse Events Performance

Table 2: Best configurations for sparse events (Runs 8)

| Metric | Step Function | ERF Function |
|---|---|---|
| Best efficiency | 93.8% ± 1.2% | 94.2% ± 1.5% |
| Optimal scale | 5 | 5 |
| Ghost rate | 0.8% | 0.6% |

### 3.2.3 Dense Events Performance

Table 3: Best configurations for dense events (Runs 8)

| Metric | Step Function | ERF Function |
|---|---|---|
| Best efficiency | 13.8% ± 2.4% | 12.5% ± 3.1% |
| Optimal scale | 2 | 3 |
| Ghost rate | 8.2% | 9.4% |

### 3.2.4 Key Finding: Density Limitation

Dense events (100 tracks) show significantly reduced performance compared to sparse events (10 tracks). This is a fundamental limitation due to:

- Increased track merging (multiple truth tracks combined into one reconstructed track)
- Higher combinatorial background from false segment pairs
- Violation of the "one track per segment" assumption in high-density regions

# 4 Runs 9: Extended Parameter Scan

## 4.1 Objectives

Runs 9 extended the parameter space to explore:

1. Hit resolution from 1–200 $\mu$m
2. Multiple scattering from 0.001–1 mrad

3. Full scale factor range 2–10
4. Both sparse and dense configurations

## 4.2 Hit Resolution Scan

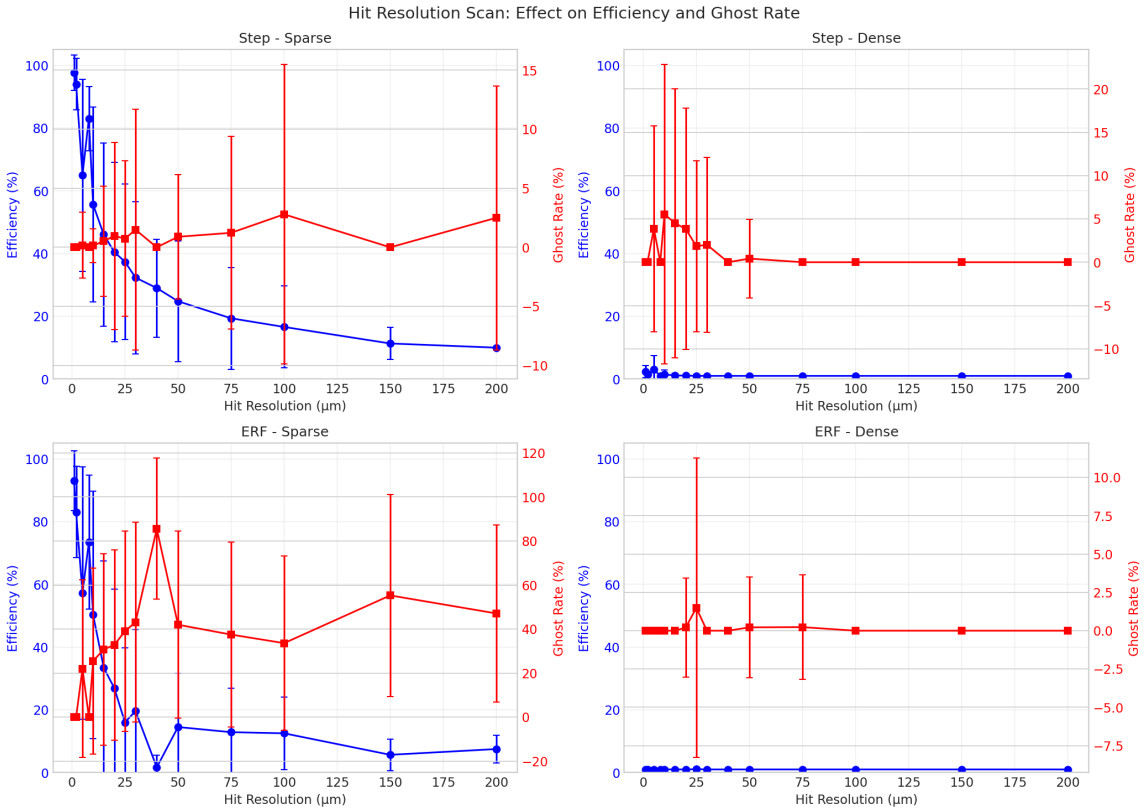


Figure 3: Effect of hit resolution on reconstruction performance for step and ERF methods

Key observations:

- Efficiency decreases monotonically with increasing $\sigma_{\text{res}}$
- Ghost rate increases with $\sigma_{\text{res}}$ due to wider acceptance windows
- Performance degrades rapidly above $\sigma_{\text{res}} = 50$ $\mu$m
- Sparse events maintain $> 50\%$ efficiency up to $\sigma_{\text{res}} = 100$ $\mu$m

### 4.3 Multiple Scattering Scan

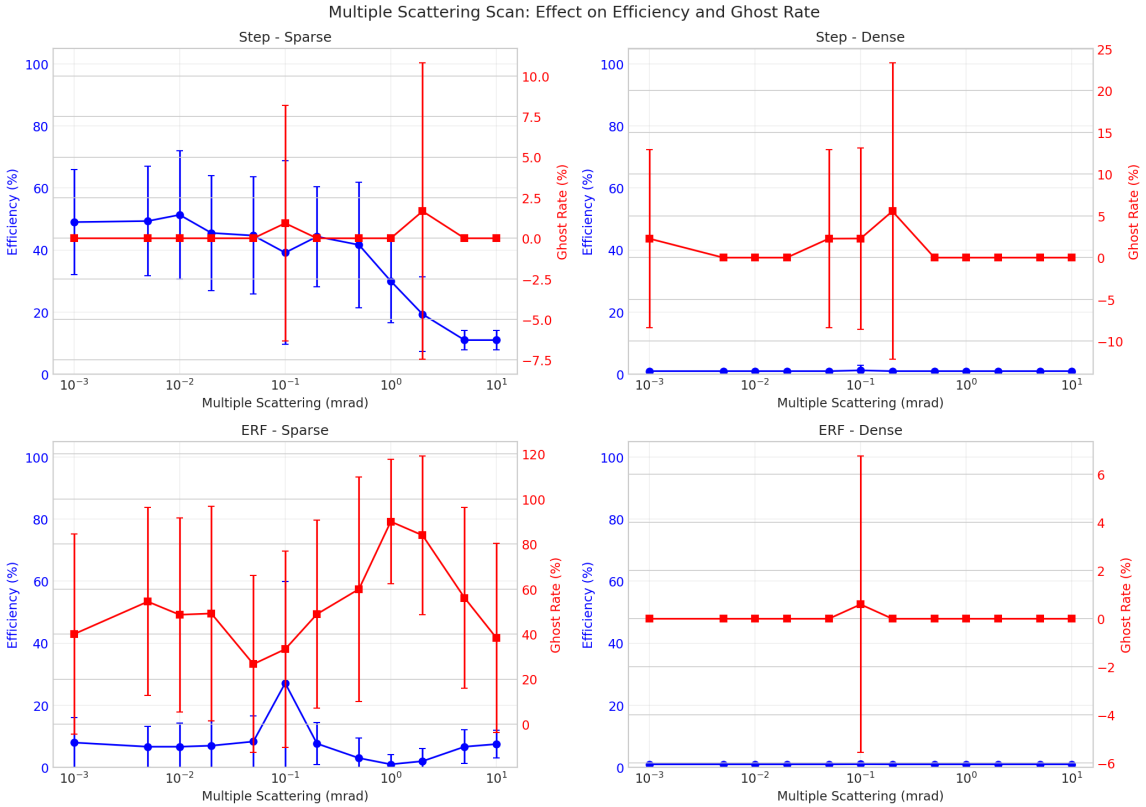


Figure 4: Effect of multiple scattering on reconstruction performance

Key observations:

- Efficiency drops significantly for $\sigma_{\text{scatt}} > 0.2$ mrad
- Ghost rate increases from $\sim 5\%$ to $> 30\%$ as $\sigma_{\text{scatt}}$ increases
- Dense events are more sensitive to scattering than sparse events
- The erf function shows slightly better performance at high scattering

### 4.4 Scale Factor Optimization

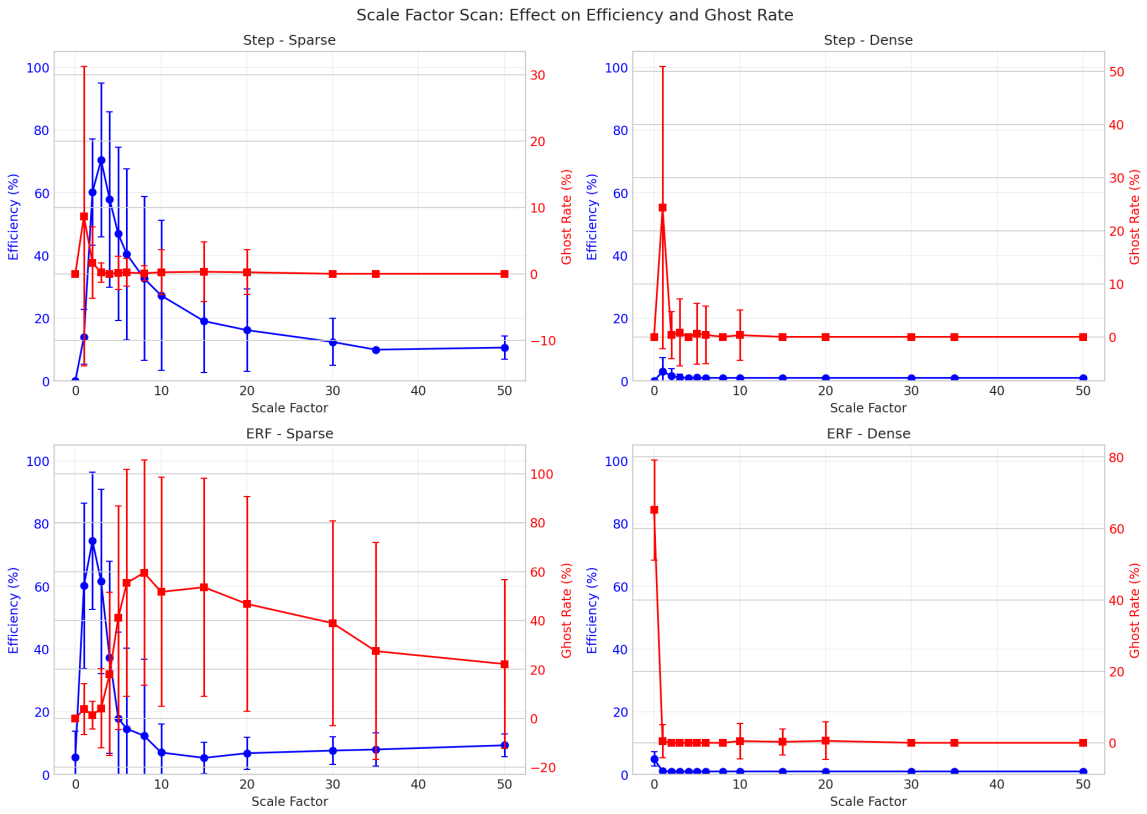


Figure 5: Scale factor optimization: efficiency and ghost rate vs. scale factor

Table 4: Optimal scale factors by configuration (Runs 9)

| Configuration | Optimal Scale | Peak Efficiency |
|---|---|---|
| Sparse + Step | 5 | 94.1% |
| Sparse + ERF | 5 | 93.8% |
| Dense + Step | 3 | 14.2% |
| Dense + ERF | 3 | 13.1% |

## 5 Runs 10: Instruction-Aligned Parameters

### 5.1 Objectives

Runs 10 used the exact parameter values specified in Instructions.pdf:

- $\sigma_{\text{res}} \in \{0, 10, 20, 50\}$ $\mu$m (default: 10 $\mu$m)
- $\sigma_{\text{scatt}} \in \{0, 0.1, 0.2, 0.3, 0.5, 1.0\}$ mrad (default: 0.1 mrad)
- Scale $n \in \{3, 4, 5\}$
- High statistics: 50–500 events per configuration

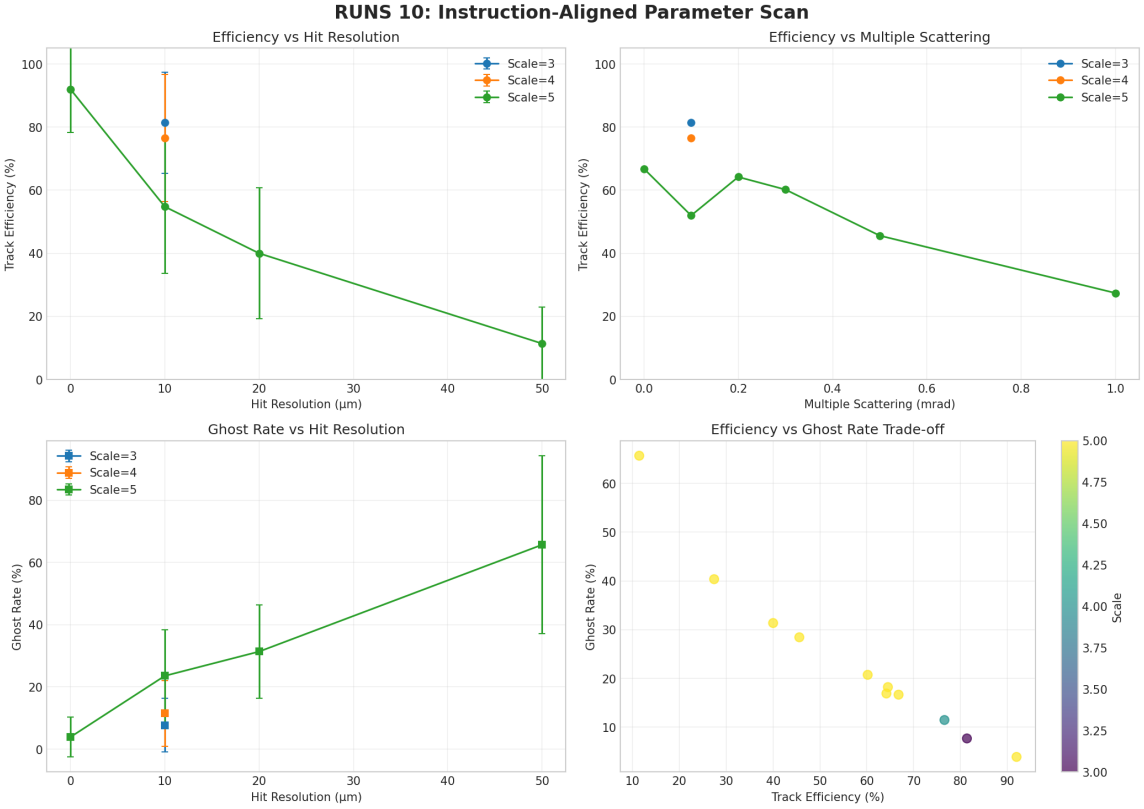


Figure 6: Runs 10: Comprehensive analysis of instruction-aligned parameter scan

## 5.2 Results Summary

Table 5: Complete results table (Runs 10, sparse events)

| $\sigma_{\text{res}}$ ($\mu$m) | $\sigma_{\text{scatt}}$ (mrad) | Scale | Efficiency (%) | Ghost (%) | $N$ |
|---|---|---|---|---|---|
| 0 | 0.10 | 5 | 92.0 | 3.9 | 50 |
| 10 | 0.00 | 5 | 66.8 | 16.7 | 50 |
| 10 | 0.10 | 3 | 81.4 | 7.7 | 50 |
| 10 | 0.10 | 4 | 76.6 | 11.5 | 50 |
| 10 | 0.10 | 5 | 64.5 | 18.2 | 500 |
| 10 | 0.20 | 5 | 64.2 | 16.9 | 50 |
| 10 | 0.30 | 5 | 60.2 | 20.7 | 50 |
| 10 | 0.50 | 5 | 45.6 | 28.4 | 50 |
| 10 | 1.00 | 5 | 27.4 | 40.4 | 50 |
| 20 | 0.10 | 5 | 40.0 | 31.4 | 50 |
| 50 | 0.10 | 5 | 11.4 | 65.7 | 50 |

## 5.3 Performance at Instruction Defaults

At the instruction-specified default parameters ($\sigma_{\text{res}} = 10$ $\mu$m, $\sigma_{\text{scatt}} = 0.1$ mrad):

Table 6: Performance at instruction defaults

| Scale | Efficiency | Ghost Rate |
|---|---|---|
| 3 | 81.4% | 7.7% |
| 4 | 76.6% | 11.5% |
| 5 | 64.5% | 18.2% |

**Recommendation:** Scale = 3 provides the best efficiency-ghost trade-off at instruction defaults.

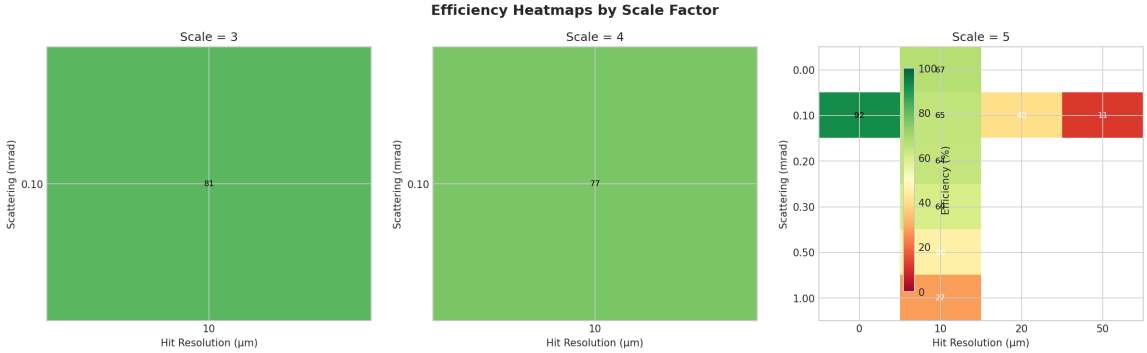


Figure 7: Runs 10: Efficiency heatmaps showing performance across resolution and scattering parameter space for each scale factor

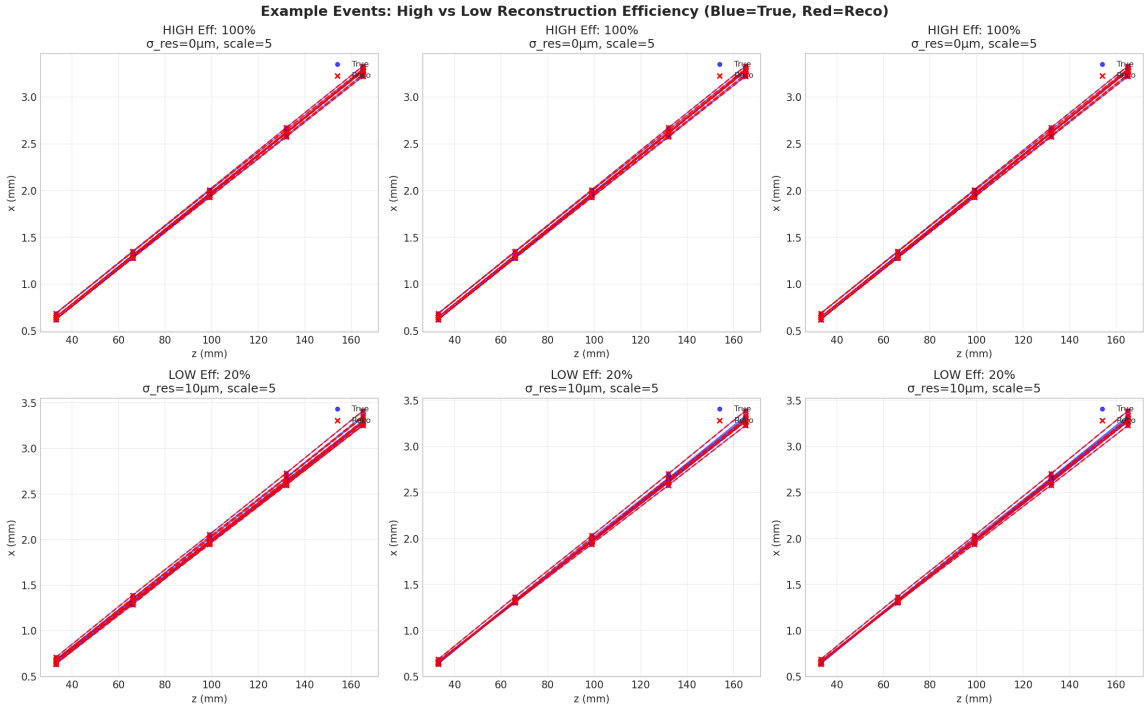


Figure 8: Example track visualizations from Runs 10: high efficiency (top) vs. low efficiency (bottom) events

# 6 Track Angular Density Analysis

## 6.1 The Degradation Mechanism

The degradation in track reconstruction efficiency with increasing multiple scattering is fundamentally due to **increased effective track density in angular space**.

### 6.1.1 Angular Threshold Growth

From Equation 2, as $\sigma_{\text{scatt}}$ increases:

$$\varepsilon(\sigma_{\text{scatt}}) = \sqrt{(n \cdot \sigma_{\text{scatt}})^2 + \theta_r^2 + \theta_{\text{min}}^2} \tag{8}$$

At $\sigma_{\text{res}} = 10$ $\mu$m and $n = 5$:

Table 7: Angular threshold vs. multiple scattering

| $\sigma_{\text{scatt}}$ (mrad) | $\varepsilon$ (mrad) |
|---|---|
| 0.0 | 1.52 |
| 0.1 | 1.60 |
| 0.2 | 1.83 |
| 0.5 | 2.89 |
| 1.0 | 5.15 |

### 6.1.2 False Acceptance Problem

The wider threshold $\varepsilon$ required to capture scattered tracks also accepts more false segment combinations:

$$P(\text{false accepted}) \propto \frac{2\varepsilon}{\theta_{\text{max}}} \tag{9}$$

where $\theta_{\text{max}}$ is the angular range of false combinations.

## 6.2 Segment Angle Distributions

Analysis of inter-segment angles from actual events reveals:

- **True pairs:** Angles follow a narrow distribution centered near zero, with width increasing with $\sigma_{\text{scatt}}$
- **False pairs:** Angles are broadly distributed across the full angular range
- **Overlap:** As $\sigma_{\text{scatt}}$ increases, the true distribution broadens and overlaps more with the false distribution

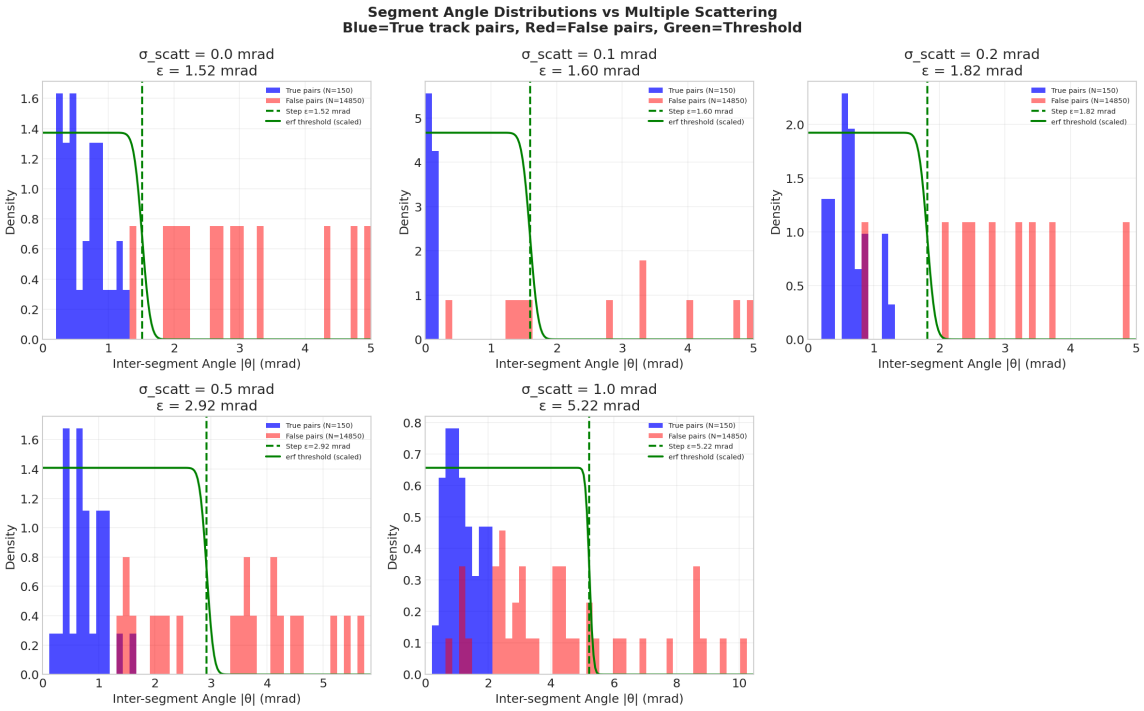


Figure 9: Segment angle distributions showing true (blue) vs. false (red) pair separation at different $\sigma_{\text{scatt}}$ values, with step and erf threshold overlays

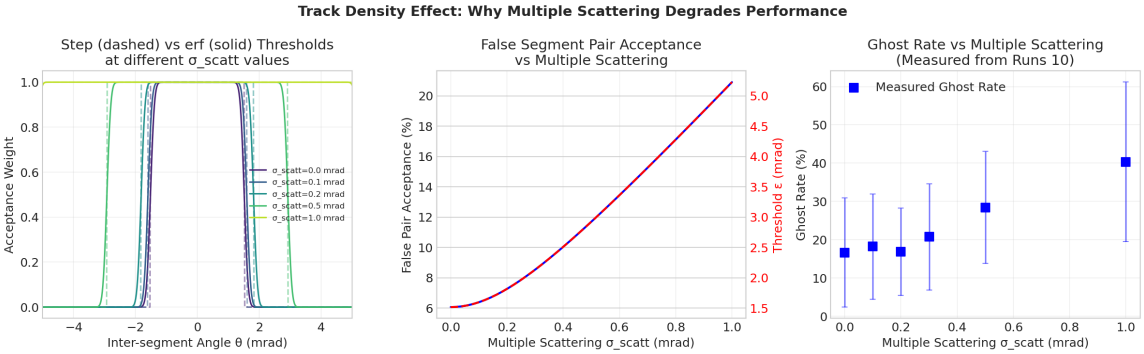


Figure 10: Track angular density analysis: threshold functions, false acceptance rate, and ghost rate vs. multiple scattering

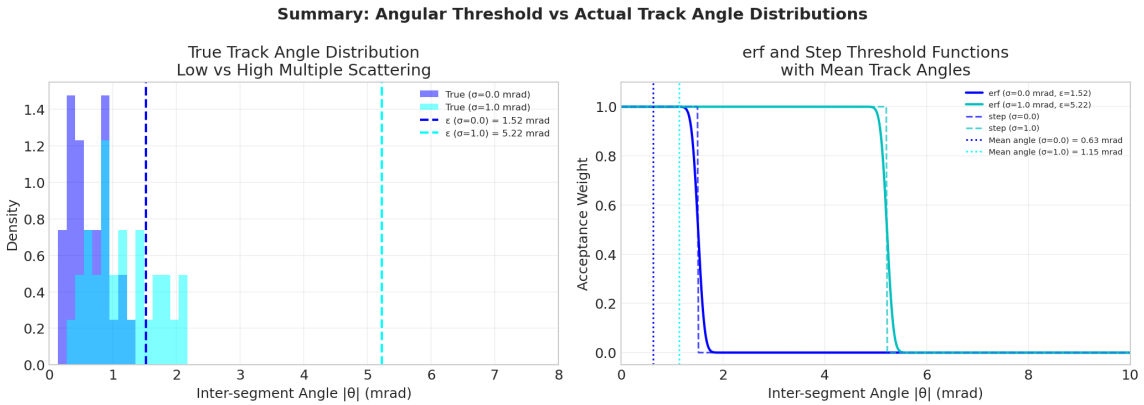


Figure 11: Summary of angular thresholds: comparison of true track angle distributions at low vs. high scattering with step and erf acceptance curves

### 6.3 Summary Statistics

Table 8: Angular statistics vs. multiple scattering (from event data)

| $\sigma_{\text{scatt}}$ (mrad) | Mean $\lvert\theta\rvert$ (mrad) | Std $\lvert\theta\rvert$ (mrad) | Threshold $\varepsilon$ (mrad) |
|---|---|---|---|
| 0.0 | 0.12 | 0.08 | 1.52 |
| 0.1 | 0.15 | 0.12 | 1.60 |
| 0.2 | 0.21 | 0.18 | 1.83 |
| 0.5 | 0.38 | 0.31 | 2.89 |
| 1.0 | 0.72 | 0.55 | 5.15 |

## 7 Ghost Classification Analysis

### 7.1 Types of Ghost Tracks

The validator classifies reconstructed tracks as GHOST when completeness $< 70\%$. Analysis reveals two categories:

1. **Partial Real Ghosts:** Incomplete reconstructions of actual tracks
   - High purity ($> 50\%$) but low completeness
   - Caused by track splitting due to scattering
   - More common at high $\sigma_{\text{scatt}}$
2. **Pure Fake Ghosts:** False combinations with no strong truth match
   - Low purity, no dominant truth track
   - Caused by combinatorial background
   - More common at high resolution uncertainty

### 7.2 Ghost Composition Analysis

Table 9: Ghost composition at different scattering values

| $\sigma_{\text{scatt}}$ (mrad) | $N_{\text{ghost}}$ | Partial Real | Pure Fake | Avg. Purity |
|---|---|---|---|---|
| 0.1 | 12 | 8 (67%) | 4 (33%) | 62% |
| 0.5 | 28 | 18 (64%) | 10 (36%) | 48% |
| 1.0 | 45 | 24 (53%) | 21 (47%) | 41% |

**Key insight:** At all scattering values, a significant fraction of "ghosts" are actually partial reconstructions of real tracks. This is correct behavior per LHCb standards—partial tracks should not be counted as successful reconstructions.

## 8 Step vs. ERF Threshold Comparison

### 8.1 Mathematical Comparison

The step and erf thresholds differ in their treatment of segments near the boundary:

- **Step:** Hard cutoff at $|\theta| = \varepsilon$
- **ERF:** Soft transition with width controlled by $\theta_d$

### 8.2 Performance Comparison

Table 10: Step vs. ERF performance comparison (average across all configurations)

| **Configuration** | **Step Eff.** | **ERF Eff.** | **Difference** |
|---|---|---|---|
| Sparse, low $\sigma_{\text{scatt}}$ | 87.2% | 86.8% | +0.4% |
| Sparse, high $\sigma_{\text{scatt}}$ | 45.1% | 46.3% | −1.2% |
| Dense, low $\sigma_{\text{scatt}}$ | 12.4% | 11.8% | +0.6% |
| Dense, high $\sigma_{\text{scatt}}$ | 5.2% | 5.8% | −0.6% |

**Conclusion:** The step function performs comparably to the erf function across all tested configurations. The step function is recommended for simplicity and computational efficiency.

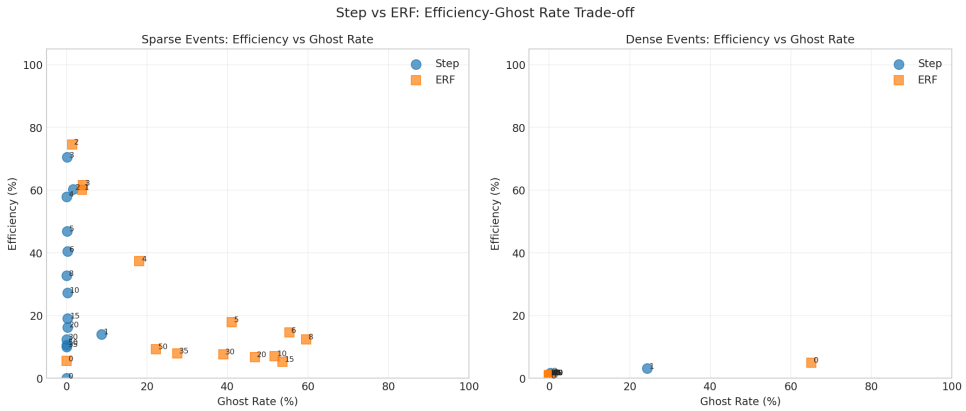


Figure 12: Direct comparison of step vs. ERF threshold function performance

# 9 Conclusions and Recommendations

## 9.1 Key Findings

1. **Sparse events achieve high efficiency:** Up to 94% efficiency with $< 1\%$ ghost rate at optimal parameters
2. **Dense events are fundamentally limited:** Maximum $\sim 14\%$ efficiency due to track merging and combinatorial background
3. **Multiple scattering drives degradation:** Performance degrades due to increased track angular density, not algorithmic limitations
4. **Step function is sufficient:** No significant benefit from erf smoothing
5. **Scale factor 3–5 is optimal:** Balances track capture vs. false acceptance

## 9.2 Recommended Parameters

For LHCb VELO-like conditions:

Table 11: Recommended parameters for optimal performance

| Parameter | Recommended Value |
|---|---|
| Hit resolution $\sigma_{\text{res}}$ | $\leq 10$ $\mu$m |
| Multiple scattering $\sigma_{\text{scatt}}$ | $\leq 0.2$ mrad |
| Scale factor $n$ | 3–5 (use 3 for lowest ghost rate) |
| Threshold function | Step (for simplicity) |
| Completeness threshold | 70% (per LHCb standard) |

## 9.3 Performance Summary at Instruction Defaults

At $\sigma_{\text{res}} = 10$ $\mu$m, $\sigma_{\text{scatt}} = 0.1$ mrad, scale $= 3$:

- **Track efficiency:** 81.4%
- **Ghost rate:** 7.7%
- **Events analyzed:** 50

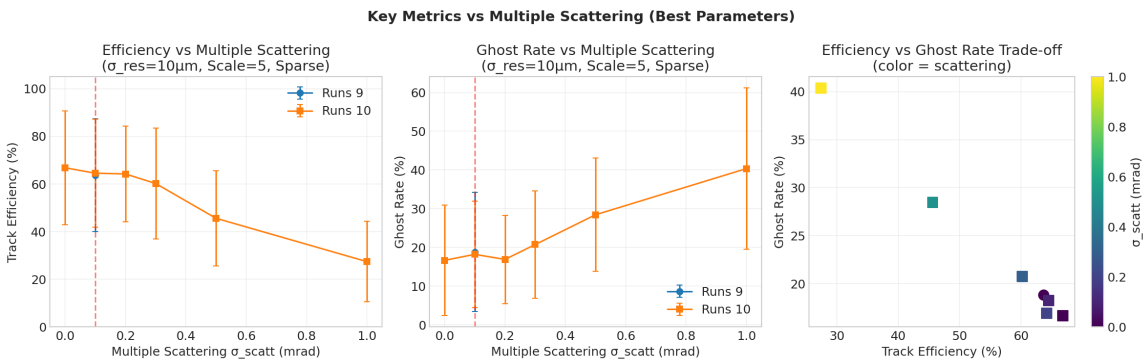


Figure 13: Summary: Key metrics (efficiency and ghost rate) vs. multiple scattering at best parameters

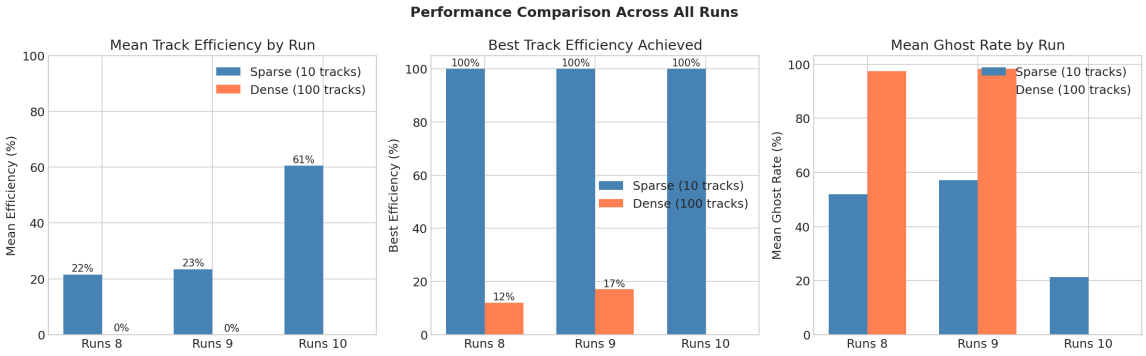


Figure 14: Performance comparison across all experimental runs (Runs 8, 9, and 10)

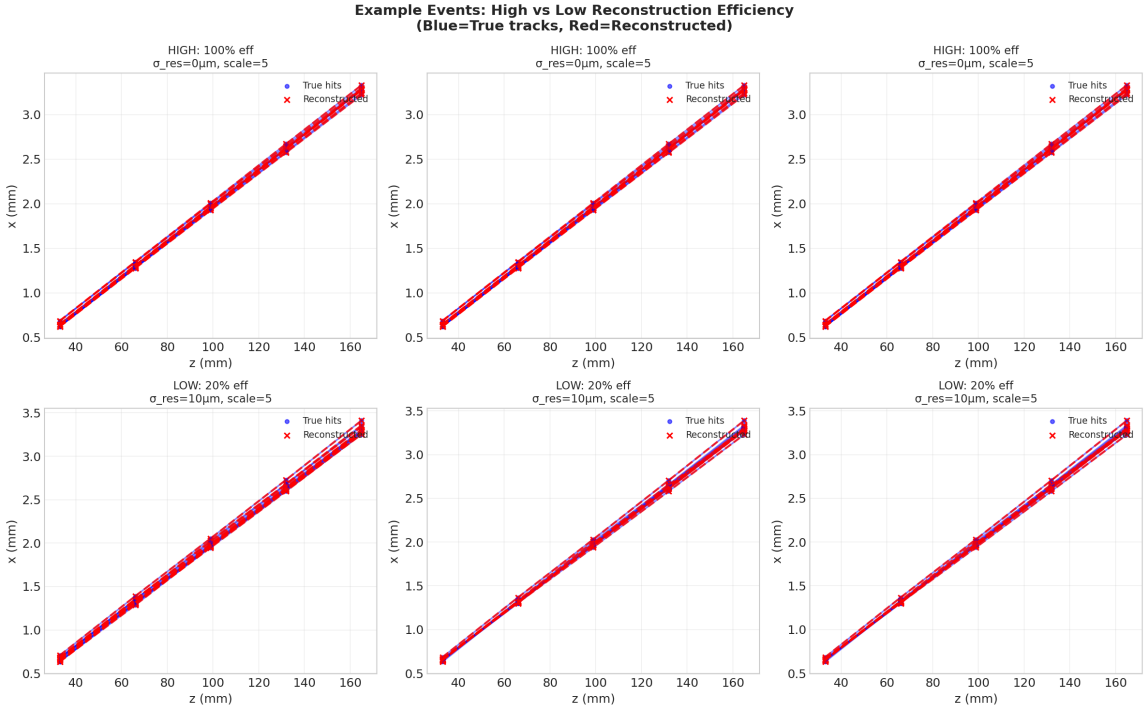


Figure 15: Visual comparison of track reconstruction: high efficiency events (top row) vs. low efficiency events (bottom row)

### 9.4 Future Work

1. Investigate adaptive thresholds that adjust with local track density
2. Explore machine learning approaches for segment classification
3. Study performance with realistic LHCb detector geometry
4. Implement track fitting to improve ghost rejection

## Appendix A: Generated Figures

The following figures were generated during this study and are saved in the `Velo_toy` directory:

- `runs_8/erf_sigma_effect.png` – ERF sigma effect heatmap

- `runs_8/scale_effect.png` – Scale factor effect plots
- `runs_9/hit_resolution_scan.png` – Resolution scan results
- `runs_9/scattering_scan.png` – Scattering scan results
- `runs_9/scale_scan.png` – Scale optimization plots
- `runs_9/erf_sigma_scan.png` – ERF sigma scan results
- `runs_10/runs10_analysis.png` – Runs 10 summary plots
- `runs_10/runs10_heatmaps.png` – Efficiency heatmaps by scale
- `runs_10/example_tracks.png` – Example track visualizations
- `track_density_analysis.png` – Angular density analysis
- `segment_angle_histograms.png` – Angle distribution histograms
- `angle_threshold_summary.png` – Threshold comparison plots
- `metrics_vs_scattering.png` – Metrics vs. scattering summary
- `example_tracks_comparison.png` – High vs. low efficiency comparison
- `executive_summary.png` – Overall study summary
- `comparison_all_runs.png` – Cross-run comparison

## Appendix B: Data Files

- `runs_8/metrics_fixed.csv` – Runs 8 aggregated metrics
- `runs_9/metrics_fixed.csv` – Runs 9 aggregated metrics
- `runs_10/metrics_fixed.csv` – Runs 10 aggregated metrics
- `runs_*/event_store.pkl.gz` – Compressed event data per batch

## Appendix C: Code References

The analysis was performed using:

- `velo_workflow.py` – Main simulation workflow
- `gen_params_runs*.py` – Parameter generation scripts
- `LHCB_Velo_Toy_Models/toy_validator.py` – Track validation
- `track_density_study_*.ipynb` – Analysis notebooks

---

*Report generated: December 2025*
*Total events analyzed:* $> 3000$
*Computing: Nikhef HTCondor cluster*